

# Neural dynamics of phoneme sequencing in real speech jointly encode order and invariant content

\*Laura Gwilliams<sup>1,2</sup>, Jean-Remi King<sup>1,3</sup>, †Alec Marantz<sup>1,2,4</sup> & †David Poeppel<sup>1,5</sup>

<sup>1</sup>Department of Psychology, New York University,

<sup>2</sup>NYU Abu Dhabi Institute,

<sup>3</sup>École normale supérieure,

<sup>4</sup>Department of Linguistics, New York University,

<sup>5</sup>Max Planck Institute

---

## Abstract

Listeners experience speech as a sequence of discrete words. However, the real input is a continuously varying acoustic signal that blends words and phonemes into one another. Here we recorded two-hour magnetoencephalograms from 21 subjects listening to stories, in order to investigate how the brain concurrently solves three competing demands: 1) processing overlapping acoustic-phonetic information while 2) keeping track of the relative order of phonemic units and 3) maintaining individuated phonetic information until successful word recognition. We show that the human brain transforms speech input, roughly at the rate of phoneme duration, along a temporally-defined representational trajectory. These representations, absent from the acoustic signal, are active earlier when phonemes are predictable than when they are surprising, and are sustained until lexical ambiguity is resolved. The results reveal how phoneme sequences in natural speech are represented and how they interface with stored lexical items.

*Keywords:* phonology, MEG, magnetoencephalography, auditory sequences, brain, language

---

## One sentence summary

The human brain keeps track of the relative order of speech sound sequences by jointly encoding content and elapsed processing time

\* Correspondence to: [leg5@nyu.edu](mailto:leg5@nyu.edu)

† Denotes equal contribution

1 Speech comprehension involves mapping non-stationary, highly variable and continuous  
2 acoustic signals onto discrete linguistic representations [1]. Although the human experience is  
3 typically one of effortless understanding, the computational infrastructure underpinning speech  
4 processing remains a major challenge for neuroscience [2] and artificial intelligence systems [3]  
5 alike.

6 Existing cognitive models primarily serve to explain the recognition of words in isolation  
7 [4, 5, 6]. Predictions of these models have gained empirical support in terms of neural encoding  
8 of phonetic features [7, 8, 9, 10], and interactions between phonetic and (sub)lexical units of  
9 representation [11, 12, 13, 14, 15]. What is not well understood, and what such models largely  
10 ignore, however, is how sequences of acoustic-phonetic signals (e.g. the phonemes *k-a-t*) are  
11 mapped to lexical items (e.g. *cat*) during comprehension of naturalistic continuous speech.

12 One substantial challenge is that naturalistic language does not come pre-parsed: there are,  
13 e.g. no reliable cues for word boundaries, and adjacent speech sounds (phonemes) acoustically  
14 overlap both within and across words due to co-articulation [1]. In addition, the same sequence  
15 of phonemes can form completely different words (e.g. *pets* versus *pest*), so preserving phoneme  
16 order is critical. Furthermore, phonemes elicit a *cascade* of neural responses, which long surpass  
17 the duration of the phonemes themselves [16, 17, 9]). This means, concretely, that a given  
18 phoneme<sub>*i*</sub> is still present in both the acoustic and neural signals while subsequent phonemes  
19 stimulate the cochlea. Such signal complexity presents serious challenges for the key goals of  
20 achieving invariance and perceptual constancy in spoken language comprehension.

21 Based on decoding analyses of acoustic and neural data we show how the brain orchestrates  
22 these overlapping inputs and overlapping neural processes, without confusing either the content  
23 or order of the phoneme sequences. We address how the language system (i) simultaneously  
24 processes acoustic-phonetic information of overlapping inputs; (ii) keeps track of the relative  
25 order of those inputs; and (iii) maintains information sufficiently long enough to interface with  
26 (sub)lexical representations.

## 27 1. Results

28 Neural responses were recorded with magnetoencephalography (MEG) while 21 participants  
29 listened to four short stories. Each subject completed two one-hour recording sessions, yielding  
30 brain responses to ~50,000 phonemes, ~10,000 words and ~1,000 sentences per subject (see  
31 Figure 1A).

### 32 1.1. Phonetic feature encoding in acoustic and neural signals

33 First we tested when and how linguistic features of the speech input are encoded in acoustic  
34 (spectro-temporal) and neural (MEG) signals. To this aim, we fit a ridge regression to decode  
35 14 phonetic features (one-hot encoding of three distinctive features *place*, *manner* and *voicing*),  
36 either from 50 frequency bands of the acoustic spectrogram (acoustic analysis) or from the 208  
37 MEG channels (neural analysis). Using a 25-split cross validation loop, the model was trained  
38 on responses to all phonemes from the training set, and then tested as a function of their relative  
39 position in the words.

40 Figure 1B shows the outcome of these analyses. Although the average phoneme duration is  
41 less than 80 ms (mean duration = 78 ms; SD = 34 ms), phonetic features (averaged over position)  
42 can be decoded from the acoustic signal between 0-300 ms ( $p < .001$ ;  $\hat{t} = 9.56$ ), and between  
43 50-300 ms in the neural signal ( $p < .001$ ;  $\hat{t} = 3.61$ ). This confirms that featural cues extend

44 to neighbouring phonemes. The ability to decode such phonetic features from the spectrum of  
 45 the acoustics shows the existence of putatively invariant acoustic cues, which sufficiently generalise  
 46 across phoneme locations [18, 19]. Furthermore, phonetic features that were more strongly  
 47 encoded in the acoustic signal were also better decoded from the neural signal (Spearman correlation  
 48  $r = .59$ ;  $p = .032$ ; note that the large difference in decoding accuracy between acoustic and  
 49 brain signals is expected given the signal-to-noise ratio of single-trial MEG recordings).

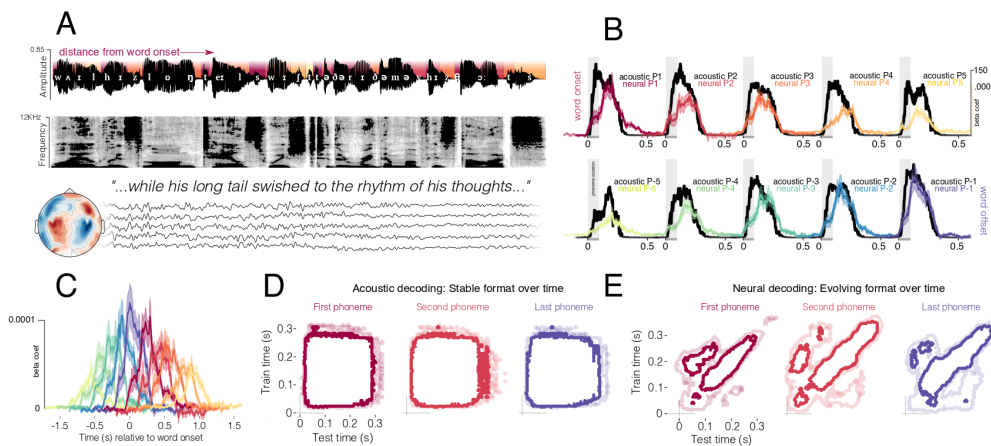


**Figure 1: Experimental design and acoustic-phonetic analysis.** A: Example sentence from the stories, with the parse into phonological units superimposed on the acoustic waveform. Colours of the segments at the top half of the waveform indicate the phoneme's distance from the beginning of a word (darker red at word onset). The spectrogram of the same sentence appears below the waveform. Five example sensor time-courses are shown below, indicating that all recordings of the continuous stories were recorded with continuous concurrent MEG. B: Time-course of phonetic-feature decoding accuracy. Black lines show accuracy of decoding features from the acoustic spectrogram. Coloured lines show results when decoding the same features from the MEG sensors. Shading in the neural data corresponds to the standard error of the mean across subjects. Results are plotted separately for 10 different phoneme positions, where P1:P5 indicates distance from word onset and P-1:P-5 distance from word offset. All plots share the same y-axis scales, which are different for neural and acoustic analyses (top right). C: The same neural decoding data are here overlaid, relative to the average duration between one phoneme and the next (around 80 ms). Multiple phonemes can be read out from the neural signal at the same time. D: Results of the temporal generalisation (TG) analysis on the acoustic data. The y-axis corresponds to the time that the decoder was trained, relative to phoneme onset; the x-axis corresponds to the time that the decoder was tested, relative to phoneme onset. The results are shown separately for three different phoneme positions. Contours represent 95% and 90% percentile decoding accuracy. E: Results of the same TG analysis applied to the MEG data, showing a very different dynamic profile from the acoustic analysis. Contours represent 95% and 90% percentile decoding accuracy.

### 50 1.2. Rapidly evolving neural representations

51 On average, phonetic features were linearly decodable for three times longer than the duration  
 52 of the phoneme itself. This suggests that, at any one time, three phonemes are being processed  
 53 concurrently (Figure 1C). How does the brain implement this set of parallel computations and  
 54 prevent interference between the resulting content?

55 We tested whether the pattern of neural activity (from the MEG analysis) or the combination  
 56 of spectro-temporal features (from the acoustic analysis) remained stable with respect to discrim-  
 57 inability using temporal generalisation analysis [20]. This reveals whether a given representation  
 58 evolves or is transformed during processing.

59 For the acoustic analysis (Figure 1D), there was significant generalisation, leading to no sta-  
60 tistical differences between the accuracy time-course of a single decoder, as compared to inde-  
61 pendent decoders at each time sample ( $p = .51$ ;  $\hat{\tau} = -.67$ ). This ‘square’ temporal generalisation  
62 suggests that although the acoustic signals are transient and dynamic, they contain stationary  
63 cues for acoustic-phonetic features. By contrast, the underlying representations of neural in-  
64 formation evolved rapidly over time (Figure 1E). Concretely, any particular topographic pattern  
65 was informative to read out a phonetic feature for around 80 ms, whereas the duration of the  
66 entire dynamic process lasted around 300 ms. This was confirmed using an independent samples  
67 t-test, comparing diagonal and horizontal decoding performance ( $p < .001$ ;  $\hat{\tau} = 7.54$ ). Neural and  
68 acoustic dynamics did not change as a function of phoneme position.  
69 Practically speaking, that the neural responses show a diagonal rather than square generali-  
70 sation pattern means the underlying activations are evolving over time: activity supporting the  
71 processing of a particular phonetic feature is either moving across cortical regions or evolving or  
72 transforming within a particular cortical region.

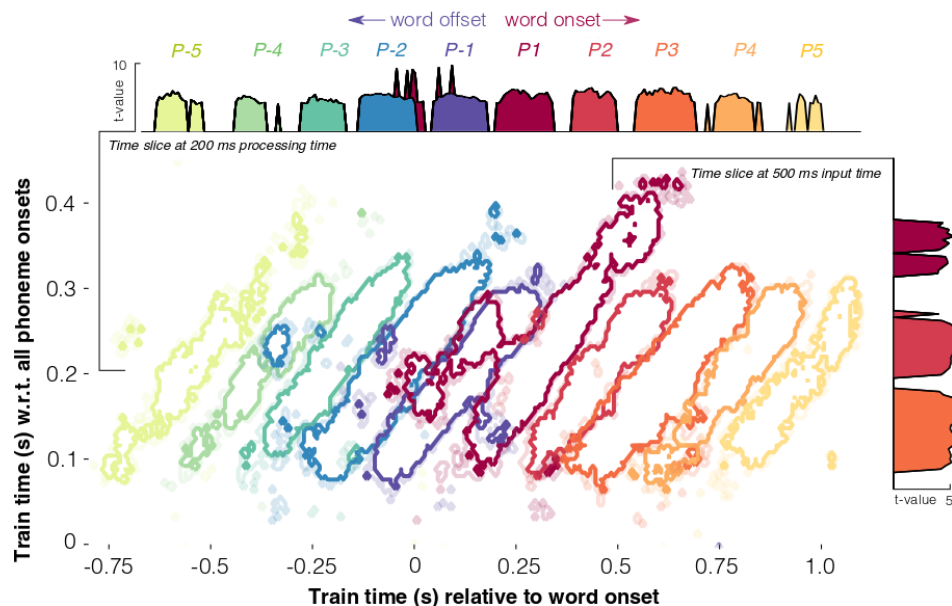


Figure 2: **Phonetic feature processing across the sequence.** Temporal generalisation (TG) results superimposed for 10 phoneme positions. From word onset (P1, dark red), and from word offset (P-1, dark blue). The result for each phoneme position is shifted by the average duration from one phoneme to the next. The y-axis corresponds to the time that the decoder was trained, relative to phoneme onset. The x-axis corresponds to the time that the decoder was tested, relative to (superimposed) word onset. Contours represent a t-value threshold of 4 (darker lines) and 3.5 (lighter lines). The panel at the top shows the t-values for each phoneme at a training time of 200 ms, showing that there is no representational overlap between neighbouring phonemes. The panel on the right shows a slice of time at 500 ms after the onset of the first phoneme. This shows that at a single moment relative to input time, multiple (at least three) phonemes can be read out of the neural responses.

73 *1.3. Phonetic sequence processing*

74 The above results show that while multiple phonemes are represented simultaneously in the  
75 brain, their dynamic encoding scheme may minimise the overlap between neighbouring repre-  
76 sentations. To test this hypothesis, we aligned the temporal generalisation matrices relative to the  
77 average latency between two adjacent phonemes. For example, relative to word onset, phoneme  
78 P1 is plot at  $t=0$ , P2 at  $t=80$ , P3 at  $t=160$ , etc. We extracted the time-samples that exceeded a  $p <$   
79  $.05$  threshold, Bonferroni-corrected across the 201 time-samples of a single processing time. We  
80 then computed the relative overlap between the time-samples of one phonemic unit and another.  
81 As shown in Figure 2, there is virtually no overlap when the data are examined at a particular  
82 processing time (horizontal axis). Crucially, this suggests that although multiple phonemes are  
83 processed in parallel, any given pattern of neural activity only represents one phoneme at a time,  
84 allowing each phoneme an individuated representation.

85 *1.4. Representations are stable for the phoneme duration*

86 Although the results show a clear evolution of representational format, each underlying neural  
87 pattern remained stable for  $\sim 80$  ms, i.e. average phoneme duration. To test whether this  
88 maintenance scales with phoneme duration, we grouped trials into quartiles, and analysed brain  
89 responses to the shortest and longest phonemes ( $\sim 4500$  trials in each bin; mean duration 45 and  
90 135 ms). Phoneme duration correlated with the duration of temporal generalisation across training  
91 time: longer phonemes generalised for an average 56 ms longer than shorter phonemes ( $p =$   
92  $.005$ ;  $\hat{t} = -2.6$ ) (Figure 3A).

93 *1.5. Representations are shared across phoneme positions: invariance*

94 Next we tested whether the same representational transformation is applied regardless of  
95 phoneme position. For this, we trained a classifier on the phonetic features of word onset  
96 phonemes and then tested this decoder on responses to the second, third and last phonemes  
97 (Figure 3B). We could read out the features of all three phoneme positions from 20-270 ms ( $p <$   
98  $.001$ ;  $\hat{t} = 3.3$ ), with comparable performance, thus supporting the position-invariant encoding of  
99 phonetic features.

100 *1.6. Phonetic processing is modulated by word boundaries*

101 How does the brain interface phonemic sequences with (sub)lexical representations (mor-  
102 phemes or words)? To address this issue, we evaluated decoding performance at word bound-  
103 aries: word onset (position P1) and word offset (position P-1) separately for each family of  
104 phonetic features (place of articulation, manner, and voicing) (Figure 3C).

105 Phonetic features were decodable earlier at word onset than offset, yielding a significant  
106 difference during the first 250 ms (place:  $p = .03$ ,  $\hat{t} = 2.77$ , 84-112 ms;  $p < .001$ ,  $\hat{t} = -2.8$ , 156-  
107 240 ms; manner  $p < .001$ ,  $\hat{t} = 3.03$ , 72-196 ms;  $p = .004$ ,  $\hat{t} = 2.75$ , 220-300ms). The latency  
108 between average neural and acoustic maximum accuracy was 136 ms (SD = 13 ms) at word onset  
109 and 4 ms (SD = 13 ms) at word offset (see Figure 1B), leading to a significant difference between  
110 onset and offset phonemes averaged over phonetic features ( $t = -3.08$ ;  $p = .002$ ). Furthermore,  
111 place and voicing features were sustained in the neural signal significantly longer for phonemes  
112 at the beginning of words as compared to the end (place:  $p = .009$ ,  $\hat{t} = -3.05$ , 302-418 ms;  
113 voicing:  $p < .001$ ,  $\hat{t} = -3.76$ , 328-428 ms). This was also true when averaging over all features ( $p$   
114  $< .001$ ,  $\hat{t} = -3.79$ , 328-396 ms) (see Figures 1B and 2).

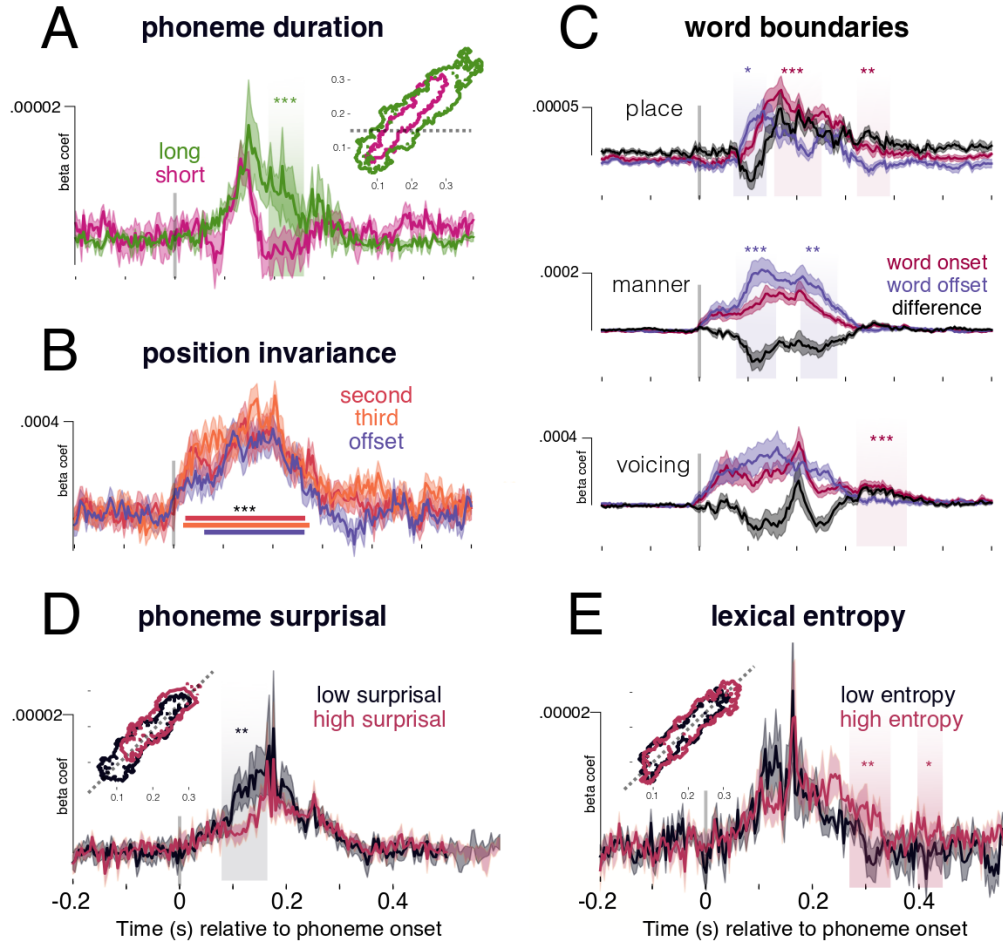


Figure 3: **Elucidating sequence dynamics.** A: TG analysis median split into short (average 45 ms) and long (average 135 ms) phonemes. Contour inlay represents the borders of the significant clusters at  $p < .001$ . Waveforms represent a horizontal slice at 140 ms (shown as a dashed line in the contour plot). B: Decoding performance when training on responses to word onset, and evaluating on second, third and last phoneme in the word. Lines represent against-chance temporal clusters exceeding  $p < .001$  for the three phoneme positions. C: Analysing responses along the diagonal plane for phonemes at word onset (dark red) and offset (dark blue) and their subtraction (black), split into the three families of phonetic features. Coloured shading corresponds to significant clusters found using applying a temporal cluster test to the difference wave. D: Analysis on all non-onset phonemes split into median surprisal, along the diagonal plane (slice shown in contour plot). Highlighted areas show significant temporal clusters between low and high surprisal. E: Analysis on all non-onset phonemes split into median cohort entropy, also along the diagonal plane. Highlighted areas show significant temporal clusters between low and high entropy. Shading on the waveform of all plots represents standard error of the mean across subjects. \* =  $p < .05$ ; \*\* =  $p < .01$ ; \*\*\* =  $p < .001$ .

115 *1.7. Predictable phonemes are processed earlier*

116 We hypothesised that the latency shift observed at word boundaries may be due to the pre-  
 117 dictability of each phoneme. Specifically, we tested whether expected phonemes could be de-



118 coded earlier from the neural signal than surprising ones. To control for co-linearity between  
119 word-boundaries and surprisal, we selected all phonemes that were *not* at word onset, and tested  
120 decoding accuracy as a function of quartile phoneme surprisal (see Methods for details on how  
121 this variable was computed). Each analysis bin contained ~4500 trials, with a mean surprisal of  
122 0.12, 1.38, 2.8 and 5.16 bits.

123 There was a systematic latency shift as a function of non-onset phoneme surprisal (Figure  
124 3D): more predictable phonemes were decoded earlier than less predictable ones, leading to a  
125 significant difference between low and high surprisal from 120-132 ms ( $p = .007$ ). Surprisal did  
126 not significantly modulate peak decoding accuracy (all uncorrected  $p$ -values  $> .2$ ).

### 127 1.8. *Phonetic features are maintained until lexical identification*

128 Finally, to investigate whether phonetic representations are maintained until word recogni-  
129 tion, we test two hypotheses: (i) phonetic features are maintained until the identification of a  
130 word boundary; or (ii) they are maintained until certainty about word identity surpasses a partic-  
131 ular threshold. We evaluated whether decoding performance between 300-420 ms (the window  
132 that showed the word onset/offset effect) was better explained by word length or by word cer-  
133 tainty (entropy over possible lexical candidates).

134 For (i), we compared decoding performance of word-onset phonemes, grouped into med-  
135 ian word length (shorter mean length = 2.54 phonemes; 4058 trials; longer mean length =  
136 5.2 phonemes; 2841 trials). No significant differences between groups were found (all clusters  $p$   
137  $> .2$ , duration  $< 2$  ms). For (ii), we grouped trials based on non-onset cohort entropy, and ran the  
138 analysis on all phonemes that did *not* occur at word onset (~4500 trials per bin, mean values of  
139 0.03, 0.77, 2.04 and 4.48 bits). In the window of interest, higher entropy phonemes we decoded  
140 with significantly higher performance (304-328 ms,  $p = .002$ ,  $\hat{t} = -2.12$ ) (see Figure 3E). This  
141 suggests that phonetic information is maintained for longer in cases of higher lexical uncertainty.

## 142 2. Discussion

143 How is the rapidly unfolding speech signal transformed into a sequence of discrete linguistic  
144 units? We analysed MEG responses to continuous speech, as a function of phonetic features  
145 and position in the phoneme sequence. Our results show that although both acoustic cues and  
146 neural processes overlap in time (lasting around 300 ms), the underlying representation evolves  
147 at the phonemic unit rate (around 80 ms), thus ensuring non-overlapping representations to avoid  
148 interference. Furthermore, we demonstrate that features are processed earlier when the phoneme  
149 is predictable – and then maintained until lexical identity is resolved. Taken together, our results  
150 show that a highly dynamic and adaptive language system underpins phonological and lexical  
151 processing during naturalistic listening.

152 The stationarity of the acoustic signal *versus* the dynamics of the corresponding neural rep-  
153 resentations highlight that speech driven-responses are more than just a reflection of the acoustic  
154 signals [21]. These dynamical representations allow the brain to process multiple (at least three)  
155 successive phonemes simultaneously, without blending them within a common activity pattern.  
156 This grants two computational advantages. First, it serves to avoid interference between phonetic  
157 units, by ensuring an orthogonal format in processing space. This answers the key question of  
158 how overlapping sequences are maintained without confusing the content of the signal. Second,  
159 relative position is implicitly coded in the representational format of each phoneme at a given  
160 input time. This allows the system to keep track of the order of speech sounds, i.e. to know that  
161 you were asked to *teach* and not *cheat*, or that you are eating *melons* and not *lemons*.

162 Building on this observation, we found that the representational trajectory is consistent across  
163 phoneme positions, thus leading to significant generalisation from one phoneme position to an-  
164 other, with comparable magnitude. Although a simple result, this rules out a number of compet-  
165 ing hypotheses. First, it is hard to reconcile these results with an explicit sequence representation.  
166 For example, if the brain represents a sequence of all elapsed phonemes, the representation of  
167 phoneme *X* at word onset would generalise poorly to third position *ABX* and even worse to sixth  
168 position *ABCDEX*. Second, under the same logic, this result rules out the idea that phonemes have  
169 a context-dependent encoding scheme, such as being represented along with their co-articulatory  
170 neighbours [22]. In that case, phoneme *X* would have a different representation in the context  
171 *AXB* and *VXY*. Finally, generalisability is inconsistent with position-specific encoding accounts,  
172 such as edge-based schemes [23, 24], which would posit that *X* is encoded differently in *ABX* and  
173 *XBC*. Instead, our results support a context-independent account, which encodes distance from  
174 phoneme onset, regardless of lexical edges.

175 If all phonemes follow a common representational trajectory relative to phoneme onset, how  
176 can we describe the transformational space? One possibility links to articulatory phonology  
177 [25]. Although we showed the input acoustic space to be (surprisingly) static, the articulatory  
178 gestures which produce those acoustics are inherently dynamic [26]. It is plausible, therefore,  
179 that speech sounds are processed via articulatory commands, which are believed to jointly encode  
180 both the sound being produced and the temporal delay relative to articulatory onset. This idea  
181 of joint content-temporal coding resonates with recent findings of sequence encoding – finding  
182 evidence for dedicated temporal codes in rat hippocampus [27]. Future work will need to further  
183 delineate the temporal code used for phonological processing, and how the spatial location of  
184 these responses changes as a function of processing time.

185 A critical finding is that the representational trajectory gets systematically delayed as a func-  
186 tion of phonological uncertainty (surprisal) and systematically sustained as a function of lexical  
187 uncertainty (cohort entropy). This suggests that the language system continuously adapts its  
188 processes based on information across multiple levels of linguistic description simultaneously.

189 The latency shift for more predictable phonemes straightforwardly aligns with models of  
190 predictive coding [28, 29] and analysis-by-synthesis [30]: when predictability for a phoneme is  
191 strong, processes can be initiated earlier (perhaps in some cases before the sensory input) than  
192 when the phoneme identity is unknown. Although previous work has shown that processing of  
193 the speech signal is sensitive to phoneme probability within a word [31, 11, 13, 14, 32], this is  
194 the first study quantifying the *consequences* this has for encoding the content of those phonemes.  
195 Interestingly, we did not observe an effect of predictability on overall decoding performance,  
196 suggesting that processing delays may serve as a compensatory mechanism to allow more in-  
197 formation to be accumulated in order to reach the same strength of encoding [33]. Future work  
198 should test whether this local (within-word) predictability metric has similar consequences to  
199 global (across-word) metrics.

200 The finding that phonetic features are maintained longer in the face of lexical ambiguity is  
201 a critical piece of the puzzle for understanding the interface between acoustic-phonetic repre-  
202 sentations and the mental lexicon. This result not only highlights the adaptivity of the speech  
203 processing system but also demonstrates the online bi-directional interaction between hierarchi-  
204 cal levels of processing. Our results suggest that acoustic-phonetic information is maintained  
205 until the (sub)lexical identity reaches a confidence threshold. To our knowledge, this is the first  
206 evidence for active maintenance of phonetic information until statistically-defined boundaries,  
207 and has clear processing advantages in the face of phonological ambiguity and lexical revision  
208 [15].



209 Overall, our results reveal that the brain implements an elegant computational solution to  
210 the processing of rapid, overlapping phoneme sequences. Namely, that the phonetic content of  
211 the unfolding speech signal is jointly encoded with elapsed processing time. Future work will  
212 need to assess the generality of this computational framework, and whether it subserves sequence  
213 processing across other modalities and domains.

### 214 3. Method

#### 215 3.1. Participants

216 Twenty-one native English participants were recruited from the NYU Abu Dhabi community  
217 (13 female; age:  $M=24.8$ ,  $SD=6.4$ ). All provided their informed consent and were compensated  
218 for their time. Participants reported having normal hearing and no history of neurological disorders.  
219 Each subject participated in the experiment twice. Time between sessions ranged from 1  
220 day to 2 months.

#### 221 3.2. Stimulus development

222 Four fictional stories were selected from the Open American National Corpus: Cable spool  
223 boy (about two bothers playing in the woods); LW1 (sci-fi story about an alien spaceship trying  
224 to find home); Black willow (about an author struggling with writer's block); Easy money (about  
225 two old friends using magic to make money).

226 Stimuli were annotated for phoneme boundaries and labels using the 'gentle aligner' from  
227 the Python module *lowerquality*. Some prior testing provided better results than the Penn Forced  
228 Aligner.

229 Each of the stories were synthesised using the Mac OSX text-to-speech application. Three  
230 synthetic voices were used (Ava, Samantha, Allison). Voices changed every 5-20 sentences. The  
231 speech rate of the voices ranged from 145-205 words per minute, which also changed every 5-20  
232 sentences. The silence between sentences randomly varied between 0-1000 ms.

#### 233 3.3. Procedure

234 Before the experiment proper, the participant was exposed to 20 seconds of each speaker  
235 explaining the structure of the experiment. This was designed to help the participants attune to  
236 the synthetic voices.

237 The order of stories was fully crossed using a Latin-square design. Participants heard the  
238 stories in the same order during both the first and second sessions.

239 Participants answered a two-choice question on the story content every ~3 minutes. For ex-  
240 ample, one of the questions was "what was the location of the bank that they robbed"? The  
241 purpose of the questions was to keep participants attentive and to have a formal measure of en-  
242 gagement. All participants performed this task at ceiling, with an accuracy of 98%. Participants  
243 responded with a button press.

244 Stimuli were presented binaurally to participants through tube earphones (Aero Technolo-  
245 gies), at a mean level of 70 dB SPL. The stories ranged from 8-25 minutes, with a total running  
246 time of ~1 hour.

247 *3.4. MEG acquisition*

248 Marker coils were placed at five positions to localise each participant's skull relative to the  
249 sensors. These marker measurements were recorded just before and after the experiment in order  
250 to track the degree of movement during the recording.

251 MEG data were recorded continuously using a 208 channel axial gradiometer system (Kanazawa  
252 Institute of Technology, Kanazawa, Japan), with a sampling rate of 1000 Hz and applying an on-  
253 line low-pass filter of 200 Hz.

254 *3.5. Preprocessing MEG*

255 The raw MEG data were noise reduced using the Continuously Adjusted Least Squares  
256 Method (CALM: (Adachi et al., 2001)), with MEG160 software (Yokohawa Electric Corporation  
257 and Eagle Technology Corporation, Tokyo, Japan).

258 The data were bandpass-filtered between 0.1 and 50 Hz using MNE-Python's default param-  
259 eters with firwin design [34] and downsampled to 250 Hz. Epochs were segmented from 200  
260 ms pre-phoneme onset to 600 ms post-phoneme onset. No baseline correction was applied. No  
261 other data cleaning was performed.

262 *3.6. Preprocessing auditory signals*

263 We computed a time-frequency decomposition of the auditory signals by applying a 100-  
264 sample Hamming window to the auditory waveform. This resulted in a power estimate at each of  
265 50 linearly spaced frequency bands from 1-11250 Hz. These data were then also downsampled  
266 to 250 Hz, and segmented from 200-600 ms in order to match the dimensionality and size of the  
267 MEG epochs.

268 *3.7. Modeled features*

269 We investigated whether single-trial sensor responses varied as a function of fourteen binary  
270 phonetic features, as derived from the multi-value feature system reported in [35]. Note that  
271 this feature system is sparse relative to the full set of distinctive features that can be identified  
272 in English; however, it serves as a reasonable approximation of the phonemic inventory for our  
273 purposes.

274 *Voicing.* This refers to whether the vocal chords vibrate during production. For example, this is  
275 the difference between *b* versus *p* and *z* versus *s*.

276 *Manner of articulation.* Manner refers to the way by which air is allowed to pass through the  
277 articulators during production. Here we tested five manner features: fricative, nasal, plosive,  
278 approximant, and vowel.

279 *Place of articulation.* Place refers to where the articulators (teeth, tongue, lips) are positioned  
280 during production. For vowels, this consists of: central vowel, low vowel, mid vowel, high  
281 vowel. For consonants, this consists of: coronal, glottal, labial and velar.

282 *Nuisance variables.* In the same model, we also accounted for variance explained by 'nuisance  
283 variables' – i.e. structural and statistical co-variables of the phonemes. Though we were not  
284 interested in interpreting the results of these features, we included them in the model to be sure  
285 that they did not account for our main analysis on the phonetic features. These features included:  
286 primary stress, secondary stress, frequency of the sequence, suffix onset, prefix onset, root onset,  
287 syllable location in the word, and syllable onset. These features were extracted from the English  
288 Lexicon Project [36].

289 *Subset variables.* Throughout the analysis, we subset trials based on their relationship to: word  
290 onset, word offset, surprisal, entropy, distance from onset, distance from offset.

291 Surprisal is given as:

$$P(w|C) = \frac{f(w)}{\sum_{w \in C} f(w)} \quad (1)$$

292 and cohort entropy is given as:

$$-\sum_{w \in C} P(w|C) \log_2 P(w|C) \quad (2)$$

293 where  $C$  is the set of all words consistent with the heard sequence of phonemes thus far, and  
294  $f(w)$  is the frequency of the word  $w$ . Measures of spoken word frequency were extracted from  
295 the English Lexicon Project [36].

### 296 3.8. Decoding

297 Decoding analyses were performed separately on the acoustic signal and on the neural signal.  
298 For the acoustic decoding, the input features were the power estimates at each of the 50 frequency  
299 bands from 1-1125 Hz. For the neural decoding, the input features were the magnitude of activity  
300 at each of the 208 MEG sensors. This approach allows us to decode from multiple, potentially  
301 overlapping, neural representations, without relying on gross modulations in activation strength  
302 [37].

303 Because some of the features in our analysis are correlated with one another, we need to  
304 jointly evaluate the accuracy of each decoding model relative to its performance in predicting  
305 all modelled features, not just the target feature of interest. This is because, if evaluating each  
306 feature independently, we will not be able to dissociate the decoding of feature  $f$  from the de-  
307 coding of the correlated feature  $\hat{f}$ . The necessity to use decoding over encoding models here,  
308 though (which, do not suffer so harshly from the problem of co-variance in the stimulus space)  
309 is one of signal to noise: we expect any signal related to linguistic processes to be contained in  
310 low-amplitude responses that are distributed over multiple sensors. Our chances of uncovering  
311 reliable responses to these features is boosted by using multi-variate models [37].

312 To overcome the issue of co-variance, but still to capitalise on the advantages of decoding  
313 approaches, we implement a back-to-back ridge regression model [38]. This involves a two  
314 stage process. First, a ridge regression model was fit on a random (shuffled) half of the data,  
315 at a single time-point. The mapping was learnt between the multivariate input (either activity  
316 across sensors or power over frequency bands) and the univariate stimulus feature (one of the 31  
317 features described above). All decoders were provided with data normalised by the mean and  
318 standard deviation in the training set:

$$\operatorname{argmin}_{\beta} \sum_i (y_i \beta^T X_i)^2 + \alpha \|\beta\|^2 \quad (3)$$

319 where  $y_i \in \{\pm 1\}$  is the feature to be decoded at trial  $i$  and  $X_i$  is the multivariate acoustic or neural  
320 measure. The l2 regularisation parameter  $\alpha$  was also fit, testing 20 log-spaced values from  $1^{-5}$  to  
321  $1^5$ . This was implemented using the *RidgeCV* function in *scikit-learn* [39].

322 Then, we use the other half of the acoustic or neural responses to generate a prediction for  
323 each of the 31 features corresponding to the test set. However, because the predictions are cor-  
324 related, we need to jointly-evaluate the accuracy of decoding each feature, to take into account

325 the variance explained by correlated non-target features. To do this, we fit another ridge regres-  
326 sion model, this time learning the beta coefficients that map the matrix of *true* feature values to  
327 *predicted* feature values:

$$\operatorname{argmin}_{\beta} \sum_i (y_i \beta^T \hat{Y}_i)^2 + \alpha \|\beta\|^2 \quad (4)$$

328 where  $y_i \in \{\pm 1\}$  is the ground truth of a particular stimulus feature at trial  $i$  and  $\hat{Y}_i$  is the prediction  
329 for all stimulus features. A new regularisation parameter  $\alpha$  was learnt for this stage. By including  
330 all stimulus features in the model, this accounts for the correlation between the feature of interest  
331 and the other features. From this, we use the beta-coefficients that map the true stimulus feature  
332 to the predicted stimulus feature.

333 The train/test split was performed 100 times, and the beta-coefficients were averaged across  
334 iterations. This circumvents the issue of unstable coefficients when modelling correlated vari-  
335 ables. These steps were applied to each subject independently.

### 336 3.9. Temporal generalisation decoding

337 Temporal generalization (TG) consists of testing whether a temporal decoder fit on a training  
338 set at time  $t$  can decode a testing set at time  $t'$  [20]. This means that rather than evaluating  
339 decoding accuracy just at the time sample that the model was trained on, we evaluate its accuracy  
340 across all possible train/testing time combinations.

341 TG can be summarised with a square training time  $\times$  testing time decoding matrix. To quan-  
342 tify the stability of neural representations, we measured the duration of above-chance generaliza-  
343 tion of each temporal decoder. To quantify the dynamics of neural representations, we compared  
344 the mean duration of above-chance generalization across temporal decoders to the duration of  
345 above-chance temporal decoding (i.e. the diagonal of the matrix versus its rows). These two  
346 metrics were assessed within each subject and tested with second-level statistics across subjects.

### 347 3.10. Comparing decoding performance between trial subsets

348 We apply analyses that rely on comparing decoding performance for different subsets of  
349 trials (e.g. between high/low surprisal, or beginning/end of word). We conduct this analysis  
350 by first training our decoding models on responses to all phonemes, thus yielding a set of fit  
351 model weights (a *topographic pattern*) at each millisecond relative to phoneme onset. We then  
352 separately evaluate the performance of these decoders on the subset trials of interest. This yields  
353 a time-course or generalisation matrix for each group of trials that we evaluate on.

### 354 3.11. Group statistics

355 In order to evaluate whether decoding performance is better than chance, we perform second-  
356 order statistics. This involves testing whether the distribution of beta coefficients across subjects  
357 significantly differs from chance (zero) across time using a one-sample permutation cluster test  
358 with default parameters specified in the MNE-Python package [34].

359 **4. Acknowledgements**

360 We thank Graham Flick for help with data collection. We are very grateful to William Id-  
361 sardi, Arianna Zuanazzi, Joan Opella, Pablo Ripolles-Vidal and Omri Raccach for their feedback  
362 on an earlier version of the manuscript. **Funding:** This project received funding from the Abu  
363 Dhabi Institute G1001 (AM); NIH R01DC05660 (DP), European Union's Horizon 2020 research  
364 and innovation program under grant agreement No 660086, the Bettencourt-Schueller Founda-  
365 tion, the Fondation Roger de Spoelberch, the Philippe Foundation (JRK) and The William Orr  
366 Dingwall Dissertation Fellowship (LG). **Author contributions:** LG: conceptualisation; method-  
367 ology; software; validation; formal analysis; investigation; data curation; writing - original draft  
368 preparation and review and editing; visualisation. JRK: conceptualisation; methodology; soft-  
369 ware; supervision. AM: conceptualisation; writing - review and editing; supervision; funding  
370 acquisition. DP: conceptualisation; writing - review and editing; supervision; funding acquisi-  
371 tion. **Competing interests:** The authors declare no competing interests. **Data and materials**  
372 **availability:** Preprocessed data will be made available after publication.

## 373 References

- 374 [1] Pisoni, D. B. & Luce, P. A. Acoustic-phonetic representations in word recognition. *Cognition* **25**, 21–52 (1987).  
375 [2] Wöstmann, M., Fiedler, L. & Obleser, J. Tracking the signal, cracking the code: Speech and speech comprehension  
376 in non-invasive human electrophysiology. *Language, Cognition and Neuroscience* **32**, 855–869 (2017).  
377 [3] Benzeghiba, M. *et al.* Automatic speech recognition and speech variability: A review. *Speech communication* **49**,  
378 763–786 (2007).  
379 [4] Marslen-Wilson, W. D. & Welsh, A. Processing interactions and lexical access during word recognition in contin-  
380 uous speech. *Cognitive psychology* **10**, 29–63 (1978).  
381 [5] McClelland, J. L. & Elman, J. L. The trace model of speech perception. *Cognitive psychology* **18**, 1–86 (1986).  
382 [6] Norris, D. Shortlist: A connectionist model of continuous speech recognition. *Cognition* **52**, 189–234 (1994).  
383 [7] Mesgarani, N., Cheung, C., Johnson, K. & Chang, E. F. Phonetic feature encoding in human superior temporal  
384 gyrus. *Science* **343**, 1006–1010 (2014).  
385 [8] Chang, E. F. *et al.* Categorical speech representation in human superior temporal gyrus. *Nature neuroscience* **13**,  
386 1428 (2010).  
387 [9] Khalighinejad, B., da Silva, G. C. & Mesgarani, N. Dynamic encoding of acoustic features in neural responses to  
388 continuous speech. *Journal of Neuroscience* **37**, 2176–2185 (2017).  
389 [10] Yi, H. G., Leonard, M. K. & Chang, E. F. The encoding of speech sounds in the superior temporal gyrus. *Neuron*  
390 **102**, 1096–1110 (2019).  
391 [11] Gwilliams, L. & Marantz, A. Non-linear processing of a linear speech stream: The influence of morphological  
392 structure on the recognition of spoken arabic words. *Brain and language* **147**, 1–13 (2015).  
393 [12] Leonard, M. K., Baud, M. O., Sjerps, M. J. & Chang, E. F. Perceptual restoration of masked speech in human  
394 cortex. *Nature communications* **7**, 1–9 (2016).  
395 [13] Gwilliams, L., Poeppel, D., Marantz, A. & Linzen, T. Phonological (un) certainty weights lexical activation. *arXiv*  
396 *preprint arXiv:1711.06729* (2017).  
397 [14] Brodbeck, C., Hong, L. E. & Simon, J. Z. Rapid transformation from auditory to linguistic representations of  
398 continuous speech. *Current Biology* **28**, 3976–3983 (2018).  
399 [15] Gwilliams, L., Linzen, T., Poeppel, D. & Marantz, A. In spoken word recognition, the future predicts the past.  
400 *Journal of Neuroscience* **38**, 7585–7599 (2018).  
401 [16] Picton, T. W., Woods, D. L., Baribeau-Braun, J. & Healey, T. M. Evoked potential audiometry. *J Otolaryngol* **6**,  
402 90–119 (1977).  
403 [17] Näätänen, R. & Picton, T. The n1 wave of the human electric and magnetic response to sound: a review and an  
404 analysis of the component structure. *Psychophysiology* **24**, 375–425 (1987).  
405 [18] Stevens, K. N. & Blumstein, S. E. Invariant cues for place of articulation in stop consonants. *The Journal of the*  
406 *Acoustical Society of America* **64**, 1358–1368 (1978).  
407 [19] Blumstein, S. E. & Stevens, K. N. Acoustic invariance in speech production: Evidence from measurements of  
408 the spectral characteristics of stop consonants. *The Journal of the Acoustical Society of America* **66**, 1001–1017  
409 (1979).  
410 [20] King, J. & Dehaene, S. Characterizing the dynamics of mental representations: the temporal generalization method.  
411 *Trends in cognitive sciences* **18**, 203–210 (2014).  
412 [21] Daube, C., Ince, R. A. & Gross, J. Simple acoustic features can explain phoneme-based predictions of cortical  
413 responses to speech. *Current Biology* **29**, 1924–1937 (2019).  
414 [22] Wickelgren, W. A. Short-term memory for phonemically similar lists. *The American Journal of Psychology* **78**,  
415 567–574 (1965).  
416 [23] Glasspool, D. W. & Houghton, G. Serial order and consonant–vowel structure in a graphemic output buffer model.  
417 *Brain and language* **94**, 304–330 (2005).  
418 [24] Fischer-Baum, S. A common representation of serial position in language and memory. In *Psychology of Learning*  
419 *and Motivation*, vol. 68, 31–54 (Elsevier, 2018).  
420 [25] Ohala, J. J., Browman, C. P. & Goldstein, L. M. Towards an articulatory phonology. *Phonology* **3**, 219–252 (1986).  
421 [26] Browman, C. P. & Goldstein, L. Articulatory gestures as phonological units. *Phonology* **6**, 201–251 (1989).  
422 [27] MacDonald, C. J., Lepage, K. Q., Eden, U. T. & Eichenbaum, H. Hippocampal “time cells” bridge the gap in  
423 memory for discontinuous events. *Neuron* **71**, 737–749 (2011).  
424 [28] Sohoglu, E., Peelle, J. E., Carlyon, R. P. & Davis, M. H. Predictive top-down integration of prior knowledge during  
425 speech perception. *Journal of Neuroscience* **32**, 8443–8453 (2012).  
426 [29] Bendixen, A., Scharinger, M., Strauss, A. & Obleser, J. Prediction in the service of comprehension: modulated  
427 early brain responses to omitted speech segments. *Cortex* **53**, 9–26 (2014).  
428 [30] Halle, M. & Stevens, K. Speech recognition: A model and a program for research. *IRE transactions on information*  
429 *theory* **8**, 155–159 (1962).



- 430 [31] Gagnepain, P., Henson, R. N. & Davis, M. H. Temporal predictive codes for spoken words in auditory cortex.  
431 *Current Biology* **22**, 615–621 (2012).
- 432 [32] Di Liberto, G. M., Wong, D., Melnik, G. A. & de Cheveigné, A. Low-frequency cortical responses to natural  
433 speech reflect probabilistic phonotactics. *Neuroimage* **196**, 237–247 (2019).
- 434 [33] Gold, J. I. & Shadlen, M. N. The neural basis of decision making. *Annual review of neuroscience* **30** (2007).
- 435 [34] Gramfort, A. *et al.* Mne software for processing meg and eeg data. *Neuroimage* **86**, 446–460 (2014).
- 436 [35] King, S. & Taylor, P. Detection of phonological features in continuous speech using neural networks (2000).
- 437 [36] Balota, D. A. *et al.* The english lexicon project. *Behavior research methods* **39**, 445–459 (2007).
- 438 [37] King, J.-R. *et al.* Encoding and decoding neuronal dynamics: Methodological framework to uncover the algorithms  
439 of cognition (2018).
- 440 [38] King, J.-R., Charton, F., Lopez-Paz, D. & Oquab, M. Discriminating the influence of correlated factors from  
441 multivariate observations: the back-to-back regression. *bioRxiv* (2020).
- 442 [39] Pedregosa, F. *et al.* Scikit-learn: Machine learning in python. *Journal of machine learning research* **12**, 2825–2830  
443 (2011).